Available online at www.sciencedirect.com
SCIENCE DIRECT®
International Journal of Thermal Sciences 42 (2003) 95–105
International Journal of Thermal Sciences
www.elsevier.com/locate/ijts

Reduction of a multiphase formulation to include a simplified flow in a semi-physical model of fire spread across a fuel bed

Albert Simeoni [a,*], Paul-Antoine Santoni [a], Michel Larini [b], Jacques-Henri Balbi [a]

[a] *ERT "Feux", SPE – CNRS UMR 6134, Campus Grossetti, Università di Corsica, BP 52, 20250 Corti, Corsica, France*
[b] *ERT "Feux", IUSTI – CNRS UMR 6595, Technopôle de Château-Gombert, 5 rue Enrico Fermi, 13458 Marseille cedex 13, France*

Received 7 March 2001; accepted 31 January 2002

Abstract

The aim of our ongoing research is to propose a forest fire simulator. To this end, we have developed a semi-physical model of fire spread that has been validated experimentally thanks to laboratory-scale pine needle bed fires under both slope and low wind conditions. This model described the physical phenomena in a simple manner while providing the main characteristics of spread. However, it did not allow to describe accurately the experimental tendency of an increasing spread rate with increasing wind velocity, particularly because of the strong assumption of considering a constant wind over the entire spreading zone. In the present study, we propose a simplified description of the flow that is coupled to our model. To proceed, we carry out the reduction of a multiphase model of reference. This reduction of the complete equations that describe the flow allows us to develop a simplified flow by considering mainly the buoyancy effect induced by combustion in the flaming zone. The results are subsequently compared to laboratory experiments under varying wind and slope conditions. A substantial improvement of the predicted rates of spread is provided.

Keywords: Fire spread modelling; Fire simulator; Multiphase model; Reduction; Semi-physical model; Diffusion-reaction; Simplified flow

1. Introduction

The devastating fires that have occurred over the last few years were always associated with strong winds (USA, Greece, Corsica, etc.). Under these circumstances, it would be very useful that fire-fighters dispose of a tool that would provide rapid and relatively accurate information concerning the spread of the fire. Such a tool must provide, under real-time, large-scale predictions of the development of a fire line on a vegetation map. In light of this, the scientific community has become increasingly involved in the modelling of forest fires and a number of approaches have emerged. Based on the classification proposed by Weber [1], three types of models can be identified. The first includes statistical models that do not take physical information into consideration [2]. The second type incorporates semi-empirical models, which are based on the principle of energy conservation but which do not distinguish between the different mechanisms of heat transfer [3]. Finally, physical models describe the various mechanisms of heat transfer and production, in order to predict fire spread [4]. Among these last models, the multiphase approach, which takes the finest mechanisms involved in fire spread into consideration, is the most complete modelling that has been developed so far [5,6]. Solving such models, however, requires very long calculation times and they are thus difficult to integrate into functional fire-fighting tools. Nevertheless, the multiphase approach can be used to improve or develop simpler models dedicated to fire spread simulators [7,8]. The ongoing goal of our research team is to develop such a simple model. Its value will reside more in its short calculation time providing the necessary information (rate of fire spread, fire front geometry and temperature field) than in its extreme accuracy. Among the different simulators which have been developed so far, the majority, including BEHAVE [9] and FARSITE [10], are based upon Rothermel's model [3], which has the disadvantage of being empirical, one-dimensional and steady. Conversely, the FIRETEC model [11], which is a transport model based on sound physics, is still inappropriate to pro-

* Correspondence and reprints.
E-mail addresses: simeoni@univ-corse.fr (A. Simeoni), santoni@univ-corse.fr (P-A. Santoni), larini@iusti.univ-mrs.fr (M. Larini), balbi@univ-corse.fr (J.-H. Balbi).

1290-0729/02/$ – see front matter
PII: S1290-0729(02)00009-1

Nomenclature

C_p	specific heat at constant pressure	$J{\cdot}kg^{-1}{\cdot}K^{-1}$	
C_f	drag forces coefficient	m^{-1}	
d	prevalence distance of the radiant heat flux	m	
$\vec{g}$	acceleration due to gravity	$m{\cdot}s^{-2}$	
k	reduced heat transfer coefficient	s^{-1}	
k_v	reduced advection coefficient		
k_v^*	constant in the k_v expression		
K	thermal diffusivity	$m^2{\cdot}s^{-1}$	
m	surface thermal mass	$J{\cdot}m^{-2}{\cdot}K^{-1}$	
$\dot{M}$	mass flux	$kg{\cdot}m^{-3}{\cdot}s^{-1}$	
p	pressure	N	
p_0	empirical radiative constant	$K^{-3}{\cdot}s^{-1}$	
P	reduced radiative coefficient	$K^{-3}{\cdot}s^{-1}$	
Q	reduced combustion enthalpy	$m^2{\cdot}K{\cdot}kg^{-1}$	
R	radiant contribution of the flame	$K{\cdot}s^{-1}$	
s	surface mass	$kg{\cdot}m^{-2}$	
t	time	s	
T	temperature	K	
$\vec{V}$	velocity	$m{\cdot}s^{-1}$	
$\vec{V}_\infty$	maximal wind velocity	$m{\cdot}s^{-1}$	
x, y, z	co-ordinate in space	m	

Greek symbols

α	volume fraction		
χ	drag forces constant		
γ	combustion time constant	s^{-1}	
δ	thickness of the fuel layer	m	
θ	angle located between the normal of the front and the direction of spread		
$\overline{\overline{\pi}}$	stress tensor in the gas	$J{\cdot}m^{-3}$	
$\vec{\Pi}$	stresses at the solid/gas interface	$J{\cdot}m^{-3}$	
ρ	density	$kg{\cdot}m^{-3}$	
ϕ	flame tilt angle		

Diacritical

[ ]	source term		

Subscripts

a	ambient		
eq	medium equivalent to the litter		
g	gaseous phase		
gk	interface exchanges		
ig	ignition		
k	solid phase		
sl	slope		
x	horizontal co-ordinate		
z	vertical co-ordinate		
0	initial condition		

vide real-time predictions. Finally, the AIOLOS-F simulator [12] seems to be the most operational existing tool.

In order to reach a compromise between rapidity and accuracy, we have developed a semi-physical model of fire spread across a fuel bed which is unsteady and two-dimensional along the ground shape [13,14]. It is based on a reaction–diffusion formulation like the one presented in [15]. In this model, we assumed that radiation is the prevailing heat transfer mechanism involved in fire spread [16]. Nevertheless, it was unable to correctly predict high wind effects on the rate of spread. Thus, we developed a theoretical method to improve it [17]. The key concept of this process, consists in reducing the multiphase model provided in [6] to obtain a thermal balance that nears our formulation. This led us to modify our model in an effort to investigate the wind-aided fire spread configurations. However, as a first step, we assumed that the wind was constant over the whole spreading zone. Thus, the generated model failed to properly describe the experimental increase in spread rate with increasing wind velocity [17]. This particular behaviour demonstrated the needs to consider the variations of gas velocity within the combustion zone.

This aspect will be considered in the present study. However, if one wants to describe completely aerodynamics, the whole set of equations governing the flow should be considered. Following our aim that consists in representing the phenomena in a simple way and according to our modelling approach [17], we have based our study on the reduction of the flow equations of the multiphase model proposed in [6]. This leads us to describe local wind variations by considering mainly the buoyancy effects induced by the combustion in the flaming zone. We thus propose to add two supplementary simplified equations to our semi-physical model, a mass balance and a momentum equation. In order to obtain these equations, we set some hypotheses, including that of a flow in the direction of the slope. Therefore, in the present study we propose a new formulation of the semi-physical model that includes a simplified description of aerodynamics in addition to the thermal balance. This new model is then used to study fire spreads over pine-needle beds under both wind and slope conditions.

The following section presents the reduction of the multiphase model we proceed to obtain the simplified flow. The formulation of the semi-physical model including the simplified flow is then presented in the third section. The fourth section is devoted to the presentation of the experimental method that was used to validate the results of simulations. Finally, the last section contains a confrontation between simulated and experimental data, and the discussion.

2. The simplified flow

Our previous semi-physical model did not provide any information concerning local wind conditions. Indeed, it

was only based on the following thermal balance (cf. Appendix A):

$$\frac{\partial T}{\partial t} + k_v \vec{V}_g \cdot \vec{\nabla} T = -k(T - T_a) + K\Delta T - Q\frac{\partial s_k}{\partial t} + R \quad (1)$$

A simplified flow based on a reduction of the multiphase approach [6] will thus be developed to determine the gas velocity $\vec{V}_g$. The model reduction is performed in two successive steps. At first, the mass balance is reduced by considering solely a flow in the direction of the slope, this assumption allows us to develop a simple equation describing local wind conditions. Furthermore, this configuration corresponds to the experimental conditions used to validate the model [18]. Secondly, as the vertical component of the gas velocity appears as a variable to be determined in the expression of the reduced mass balance equation, we simplify the multiphase momentum equation to obtain it directly from the temperature field.

2.1. Determination of the horizontal velocity

We start from the multiphase model of reference [6], by using its mass balance equation of the gas phase:

$$\frac{\partial}{\partial t}(\alpha_g \rho_g) + \vec{\nabla} \cdot (\alpha_g \rho_g \vec{V}_g) = \sum_k [\dot{M}]_{gk} \quad (2)$$

To simplify this equation, we assume that the volume fraction of the gas phase remains constant (indeed, for unburned fuel we have: $\alpha_g = 0.97 \approx 1$) and that there is only one solid phase. Furthermore, we consider that the flow is quasi-static (i.e., we assume that wind variations with respect to temperature occur infinitely faster than temperature variations with respect to wind) and follows the direction of the slope. So, Eq. (2) becomes:

$$\rho_g \frac{\partial V_{g,x}}{\partial x} + \rho_g \frac{\partial V_{g,z}}{\partial z} + V_{g,x}\frac{\partial \rho_g}{\partial x} + V_{g,z}\frac{\partial \rho_g}{\partial z} = [\dot{M}]_{gk} \quad (3)$$

Then, to consider mean values of the state variables in the fuel bed, we subsequently apply an averaging procedure along the thickness δ of the fuel bed (cf. Fig. 1) [17]. As the temperature profile is assumed in the semi-physical model as being a constant throughout the height of the litter, we obtain:

$$\frac{\partial V_{g,x}}{\partial x} + \frac{V_{g,x}}{\rho_g}\frac{\partial \rho_g}{\partial x} = -\frac{[V_{g,z}]_0^\delta}{\delta} + \frac{1}{\rho_g}[\dot{M}]_{gk} \quad (4)$$

For the sake of clarity, the symbols identifying that the variables are averaged have been omitted. We also assume that the vertical component of the gas velocity follows a boundary layer profile (i.e., $V_{g,z}(0) = 0$). We thus obtain:

$$\frac{\partial V_{g,x}}{\partial x} + \frac{V_{g,x}}{\rho_g}\frac{\partial \rho_g}{\partial x} = -\frac{V_{g,z}(\delta)}{\delta} + \frac{1}{\rho_g}[\dot{M}]_{gk} \quad (5)$$

We then have to solve this differential equation. The variables are determined in the following manner:

- The gas density is provided by the isobaric perfect gas law, since we are dealing with quasi-isobaric flames:

$$\rho_g T_g = \rho_a T_a = \text{constant} \quad (6)$$

- The mass increase in the gas phase is obtained from the sub-model of fuel mass loss, assuming that the mass lost by the vegetal is gained by the gas phase.

We therefore obtain (cf. Appendix A):

$$[\dot{M}]_{gk} = -\frac{1}{\delta}\frac{\partial s_k}{\partial t} = \frac{\gamma s_{k0}\, e^{-\gamma(t-t_{ig})}}{\delta} \quad (7)$$

In order to close the simplified flow model, we need to determine the ascensional gas velocity at the top of the fuel bed $V_{g,z}(\delta)$ present in Eq. (5).

2.2. Determination of the ascensional velocity

The multiphase momentum equation of the gas phase [6] is:

$$\frac{\partial}{\partial t}(\alpha_g \rho_g \vec{V}_g) + \vec{\nabla} \cdot (\alpha_g \rho_g \vec{V}_g \vec{V}_g) - \vec{\nabla} \cdot (\alpha_g \bar{\bar{\pi}}_g) - \alpha_g \rho_g \vec{g} = \sum_k [\dot{M}\vec{V}]_{gk} + \sum_k [\vec{\Pi}]_{gk} \quad (8)$$

By assuming, as above, that the volume fraction of the gas remains constant, that there is only one solid phase and that the flow is quasi-static, we are able to reformulate the

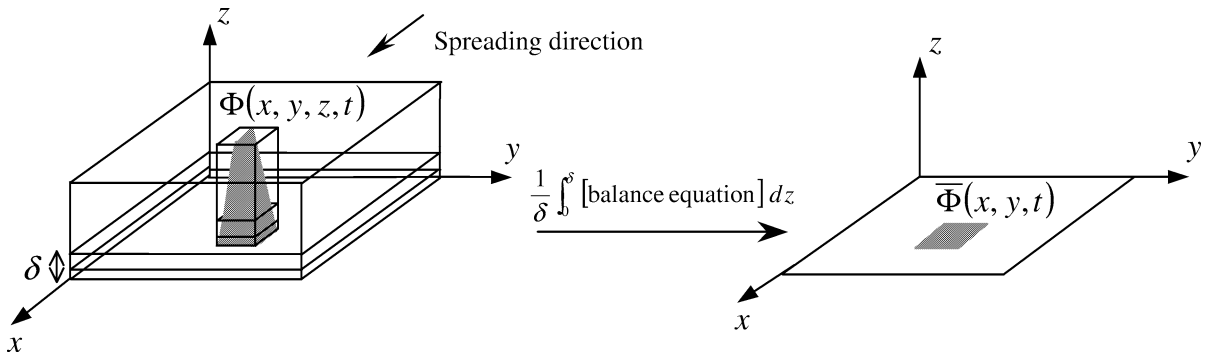

Fig. 1. The two-dimensional reduction procedure.

momentum Eq. (8) in its rotational form. We also substract the mass balance Eq. (2) to obtain:

$$\rho_g \vec{V}_g \wedge \left(\overrightarrow{\mathrm{rot}}\vec{V}_g\right) + \frac{1}{2}\rho_g \vec{\nabla}\vec{V}_g^2 = \vec{\nabla}\cdot\bar{\bar{\pi}}_g + \rho_g \vec{g} + \left[\dot{M}\vec{V}\right]_{gk} + \left[\vec{\Pi}\right]_{gk} - \vec{V}_g\left[\dot{M}\right]_{gk} \quad (9)$$

Then, we disregard the momentum sources, the shear stresses in the gas phase and we assume that the stresses at the solid/gas interface are represented solely by the drag forces. We also assume that the flow is irrotational and we set the hydrostatic pressure assumption. Thus, we obtain the following momentum equation projected onto the vertical axis:

$$\frac{\partial}{\partial z}\left(V_{g,x}^2 + V_{g,z}^2\right) = 2\left(\frac{\rho_a}{\rho_g} - 1\right) g\cos\phi_{sl} - C_f V_{g,z}^2 \quad (10)$$

This relationship implies that the vertical velocity only depends on the buoyancy and drag force effects, and that the other effects are negligible [19]. We then have to apply the averaging procedure along δ, while assuming that the profile of the vertical component of velocity is linear in the fuel bed. This generates:

$$\frac{1}{\delta}\int_0^\delta V_{g,z}^2\,\mathrm{d}z = \frac{1}{3}V_{g,z}^2(\delta) \quad (11)$$

We therefore have (without any average symbol):

$$\frac{1}{\delta}\left[V_{g,x}^2 + V_{g,z}^2\right]_0^\delta = 2\left(\frac{\rho_a}{\rho_g} - 1\right) g\cos\phi_{sl} - \frac{C_f}{3}V_{g,z}^2(\delta) \quad (12)$$

We set an additional hypothesis concerning the velocity in order to extensively simplify our equation. We assume that the profile of the horizontal component of velocity is constant along the thickness of the litter. So, the isobar perfect gas law allows to obtain the following relation:

$$V_{g,z}(\delta) = \chi\sqrt{2\delta\left(\frac{T_g}{T_a} - 1\right) g\cos\phi_{sl}} \quad (13)$$

with

$$\chi = \sqrt{\frac{3}{3 + \delta C_f}} \quad (14)$$

We have finally estimated coefficient C_f, based on the physical properties of pine needles [20]. To proceed, we used an empirical law which considers needles as cylinders distributed in a random manner all along the fuel bed [21]. We obtained the following estimation of coefficient χ:

$$\chi = 0.33 \quad (15)$$

The aim of this work is to demonstrate that the definition of a simplified flow allows to improve the predictions of a simple model in the configuration of wind-driven fires, while keeping a short computational time. This approach is rather original. Indeed, most of the models based on a thermal balance do not describe the flow and often assume a constant wind over the spreading zone. This wind is either considered equal to the dominant wind [22] or to a percentage of it [23]. Nevertheless, it is clear that this work represents only a step towards the simulator which requires the description of the two horizontal components of the gas velocity.

3. A semi-physical model of fire spread including a simplified flow

By coupling Eq. (1) with the simplified flow, we generate a new model that contains a thermal balance for the medium equivalent to the litter, a mass balance for the gas phase, a momentum equation along the vertical axis and the isobaric perfect gas law. This leads us to:

$$\frac{\partial T}{\partial t} + k_v \vec{V}_g\cdot\vec{\nabla}T = -k(T - T_a) + K\Delta T - Q\frac{\partial s_k}{\partial t} + R \quad (1)$$

$$\frac{\partial V_{g,x}}{\partial x} + \frac{V_{g,x}}{\rho_g}\frac{\partial \rho_g}{\partial x} = -\frac{V_{g,z}(\delta)}{\delta} - \frac{1}{\rho_g \delta}\frac{\partial s_k}{\partial t}$$

in the burning zone (5)

$$V_{g,z}(\delta) = \chi\sqrt{2\delta\left(\frac{T}{T_a} - 1\right) g\cos\phi_{sl}}$$

in the burning zone (13)

$$\rho_g T = \rho_a T_a$$

in the gaseous medium (16)

$$R = 0, \qquad s_k = s_{k0}\,\mathrm{e}^{-\gamma(t - t_{ig})}$$

for a burning cell (17)

$$R = P(\phi)\cos(\theta)T^4(x - d, y, t), \qquad s_k = s_{k0}$$

for an inert cell ahead of the front (18)

$$R = 0, \qquad s_k = s_{k0}$$

for an unburned cell somewhere else (19)

With the following boundary and initial conditions:

$$\begin{array}{ll} T = T_a & \text{at the boundaries far from the fire} \\ \vec{V}_{g,x} = \vec{V}_\infty & \text{at the inflow of the domain} \\ T(x, y, t = 0) = T_a & \text{for an unignited cell at time zero} \\ T(x, y, t = 0) = T_{ig} & \text{for an ignited cell at time zero} \end{array} \quad (20)$$

We can observe that gas density is defined by using the isobaric perfect gas law. To proceed, we set the hypothesis of the thermal equilibrium between the gas and solid phases in the fuel layer. So, we obtain the gas density directly from the temperature provided by Eq. (1).

Moreover, the validity domain of the simplified equations was limited to the combustion zone. Indeed, we developed relation (13), which provides the vertical component of the velocity at the top of the fuel bed by assuming that the buoyancy effects dominate the other effects. This hypothesis is valid only in the combustion region and the calculation of the local wind can thus only be implemented in it. Outside this zone, we assumed that horizontal velocity remains constant and is equal to the velocity obtained at the interface

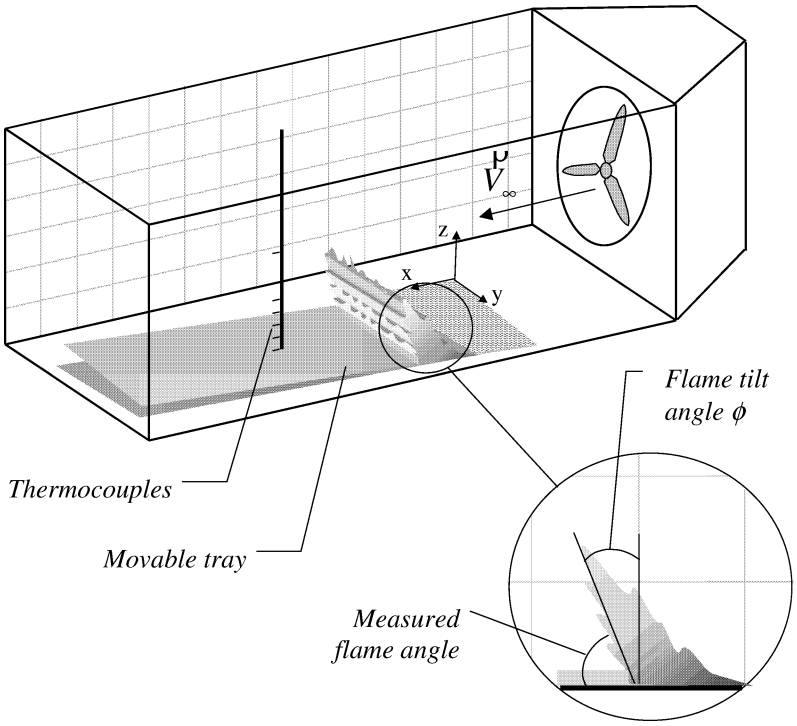

Fig. 2. Experimental wind tunnel.

between the burning and the unburned fuel. Indeed, in the burned and unburned regions, the influence of buoyancy onto the thermal transfers is assumed as becoming negligible and the other effects, as drag forces, are neglected.

4. I.S.T. experiments

4.1. Experimental set-up

These experiments were carried out in a dedicated low speed wind tunnel [18] (cf. Fig. 2). They were performed in order to observe wind driven fire across fuel beds of pine needles. Furthermore, the tunnel allows the study of both combined wind and slope effects thanks to a sloping fuel tray. The wind speed values covered the range from 0 to 3 $\mathrm{m{\cdot}s^{-1}}$ (step 1 $\mathrm{m{\cdot}s^{-1}}$) for upwind spreading. The movable tray can be set at angles from 0 up to 15° (step 5°) with upslope orientation. The fuel bed occupies the central part of the tray (0.70 m wide). It consisted of a layer of *Pinus pinaster* needles, attempting to reproduce a typical layer found in Portuguese stands, with a load of approximately 0.5 $\mathrm{kg{\cdot}m^{-2}}$ corresponding to a fuel thickness of approximately $\delta = 5$ cm on a dry weight basis and a fuel moisture content of $(10 \pm 1\%)$.

4.2. Experimental runs

The movable tray was positioned at the required angle and the wind velocity fixed at the required value. The conditioned pine needles were spread uniformly over the tray. To ensure a fast and linear ignition, a small amount of alcohol and a flame torch were used. The fuel was ignited perpendicular to the flow at the wind tunnel end (cf. Fig. 2). In order to obtain a uniform and established flame propagation, the fuel bed was ignited sufficiently far away from the work section. Three runs were carried out for each set of conditions. The experimental runs were recorded by a video camera. The rate of spread was obtained from the derivative of the curve "flame front position vs. time". Twenty to thirty images from each experimental run were analysed in order to determine the mean flame angle, which is defined as being the angle between the tray and the leading surface of the flame. Temperature measurements were taken using K type thermocouples with a 250 μm wire diameter.

5. Numerical results and discussion

5.1. Previous results

The varying experimental configurations were simulated with our two previous semi-physical formulations. In what follows, the first one which does not consider any advective transfer will be called the radiative model [16]. And the second one which includes this transfer, while assuming that the wind remains constant all along the spreading domain, will be referred to the constant-wind model [17]. The model's dynamical coefficients were determined from experimental temperature curves under slopeless and windless conditions, as explained in [13,16]. We therefore dynamically identified

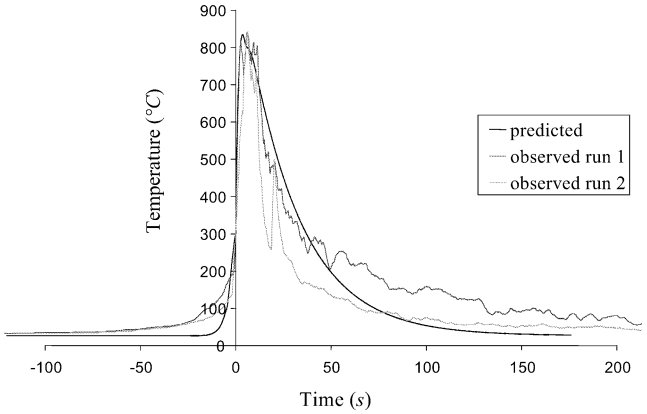

Fig. 3. Experimental and predicted temperature curves under slopeless and windless conditions.

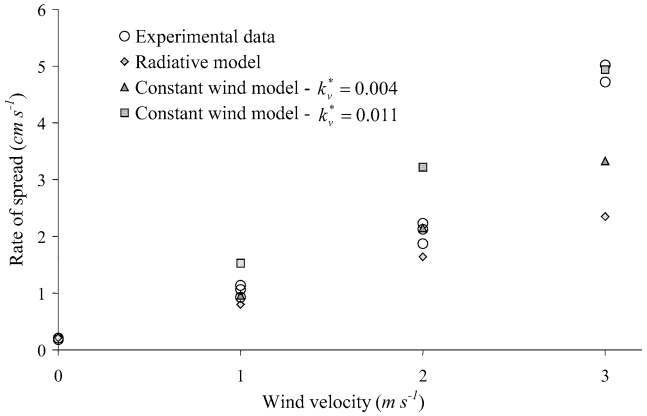

Fig. 4. Rates of spread of the radiative and the constant-wind model for no slope under various wind conditions.

the following values for the fuel considered in the IST experiments:

$$k = 97 \times 10^{-3}\ \mathrm{s}^{-1}, \qquad K = 14.5 \times 10^{-6}\ \mathrm{m}^2{\cdot}\mathrm{s}^{-1}$$
$$Q = 3.67 \times 10^{3}\ \mathrm{m}^2{\cdot}\mathrm{K}{\cdot}\mathrm{kg}^{-1}$$
$$\gamma = 0.234\ \mathrm{s}^{-1}, \qquad p_0 = 9 \times 10^{-9}\ \mathrm{K}^{-3}{\cdot}\mathrm{s}^{-1}$$

The predicted and observed temperature profiles (measured at the top of the fuel bed) are provided in Fig. 3 under slopeless and windless conditions. A general agreement was observed on the envelope of these simulated and experimental curves. We will not describe these results in detail here as they have already been discussed in Balbi et al. [13]. The predictions for both the radiative and constant–wind model are presented in Fig. 4 for no-slope conditions. With respect to the radiative model, the results corresponded to the experimental data up to a wind velocity of 1 m·s^{-1} [16]. The model was not able to accurately describe the increasing rate of spread with increasing wind velocity, however. Furthermore, the experimental values were poorly matched for the highest wind velocity of 3 m·s^{-1}. The constant-wind model allowed an improvement in the predictions. Two values for the coefficient k_v^* were necessary, however: one to correctly represent fire spread up to wind velocities of 2 m·s^{-1}, ($k_v^* = 4 \times 10^{-3}$), and a further value to represent it for the highest wind velocity of 3 m·s^{-1} ($k_v^* = 11 \times 10^{-3}$). These results illustrated the need to incorporate a simplified flow to circumvent this weakness; i.e. to keep a unique value of k_v^*, and to represent the gas velocity variations in the burning zone.

5.2. Contribution of the simplified flow

5.2.1. Numerical implementation

Following the assumption of a quasi-static flow, the system of equations was implemented in a simple manner, namely by assuming that the characteristic time of the coupled system is the one of the energy equation. Solving the equation describing local wind conditions was performed by using the 4th order Runge-Kutta method. For the thermal balance, we used a finite difference method. The mesh size was of 0.01 m whereas the time step was of 0.002 s, in order to meet the C.F.L. conditions for wind velocities of 3 m·s^{-1}. The prevalence distance of radiation was taken equal to $d = 0.01$ m. An "upwind" difference schema (finite differences in the direction of flow) was used to take into consideration the extent of convective transfers in the wind direction [24].

5.2.2. Results and discussion

Different configurations were simulated for the range of slopes previously presented and for wind velocities $\|\vec{V}_\infty\|$ of 1, 2 and 3 m·s^{-1}, in order to compare the predictions of the radiative model with the new formulation proposed here, that we will call from now on the "simplified-flow" model. The values of the coefficients k, K, Q, γ and p_0 of the model remained the same as presented previously. The value of the constant in the advection term was taken as being equal to the highest value: $k_v^* = 11 \times 10^{-3}$. Indeed, we could not use the lowest value, which under-estimated the rates of spread in the case of wind velocities of 3 m·s^{-1}.

Coefficient χ, present in Eq. (13), takes into account the influence of drag forces in the fuel layer. It represents an additional coefficient to be determined and it was estimated theoretically (cf. Section 2.2). We therefore endeavoured to examine the sensitivity of the model with respect to this coefficient. In the present paper, we will limit ourselves to a presentation and a discussion concerning the rate of fire spread as a function of this coefficient. Indeed, it represents the most relevant data (cf. Fig. 5) we can compare with experiments. Below a value of approximately $\chi = 0.5$, hot gases go through the fire front (cf. Fig. 6) and they involve an increase in the rate of spread. In addition, the value that allows us to attain the experimental rates of spread observed during the I.S.T. experiments corresponds to a coefficient $\chi = 0.25$, which is of the same order of magnitude as the estimated value ($\chi = 0.33$ in Section 2.2). It should be noted that this estimated value can only be considered as being an indication, due to the approximations made in its calculation. We subsequently used this value in all simulations, regardless of slope and wind conditions.

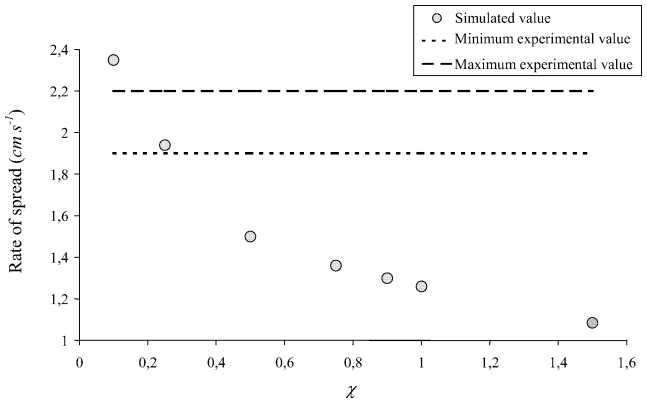

Fig. 5. Spread rate as a function of the parameter χ for a wind of 2 m·s^{-1} and no slope.

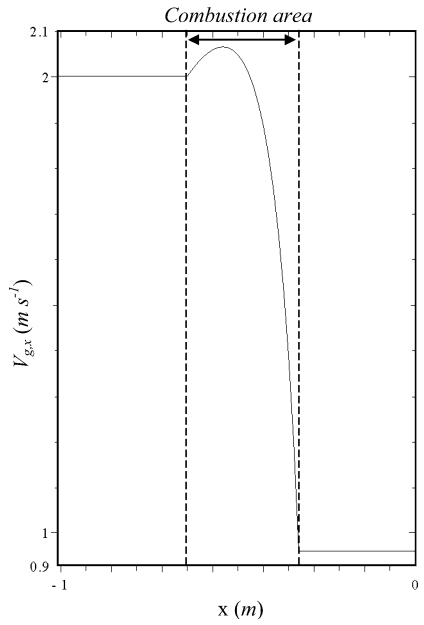

Fig. 6. Spatial distribution of horizontal velocity $V_{g,x}$ using $\chi = 0.25$ for a wind of 2 m·s^{-1} and no slope.

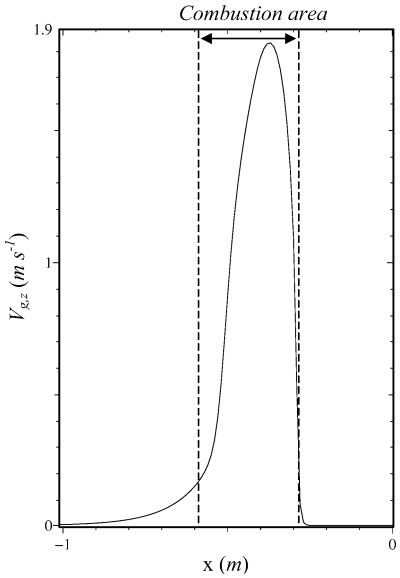

Fig. 7. Spatial distribution of the vertical velocity $V_{g,z}$ using $\chi = 0.25$ for a wind of 2 m·s^{-1} and no slope.

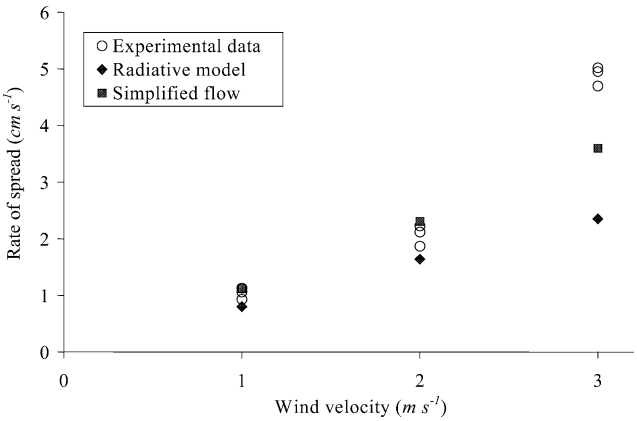

Fig. 8. Spread rate for the radiative and simplified-flow models under slopeless conditions and for various wind velocities.

This drag force coefficient allowed us to obtain the spatial distributions of the horizontal and vertical gas velocities exhibited in Figs. 6 and 7. We will only examine these results qualitatively because of the lack of gas velocity measurements in the combustion zone. Ascensional velocity (cf. Fig. 7 for a wind of 2 m·s^{-1} and zero slope) was maximal in the combustion zone and was very low outside this zone. We thus qualitatively describe the gas behaviour following its passage through the combustion zone as given by the multiphase model [25]. The variation in horizontal velocity through the combustion zone is presented in Fig. 6 for a wind of 2 m·s^{-1} and no slope. We limit ourselves to the description of a single profile here as the profiles obtained under the other experimental conditions were similar. The gas velocity exhibits a slight acceleration before penetrating the flame zone. Then, it decreases rapidly as it goes through the combustion zone, while keeping a positive value upon exiting this zone. The physical behaviour of the horizontal velocity is thus also qualitatively described. We also observed that the gases always went through the combustion zone regardless of the wind velocity entering this zone. This observation remains to be verified experimentally. We believe that one of the reasons the model behaves in this way is due to the approximated modelling of radiation, which leads us to overestimate convection when attempting to attain experimental tendencies for wind velocities of 3 m·s^{-1}. In addition, the ascensional velocity of the gas was modelled in a very simple manner and it includes a certain degree of uncertainty (when dealing with χ estimation), which could lead to an error with respect to the flow. Thus, it should be interesting to determine this velocity more accurately.

Concerning the rates of spread, Fig. 8 provides the simulated results for varying winds under no slope conditions, and Fig. 9 provides the predicted versus observed rates of spread for all the slopes and winds considered. We observe

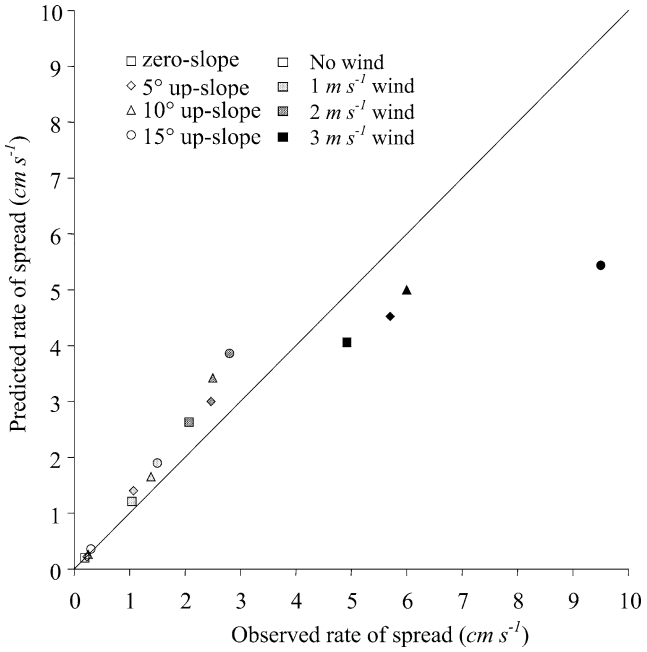

Fig. 9. Predicted versus observed rates of spread for all of the experiments carried out.

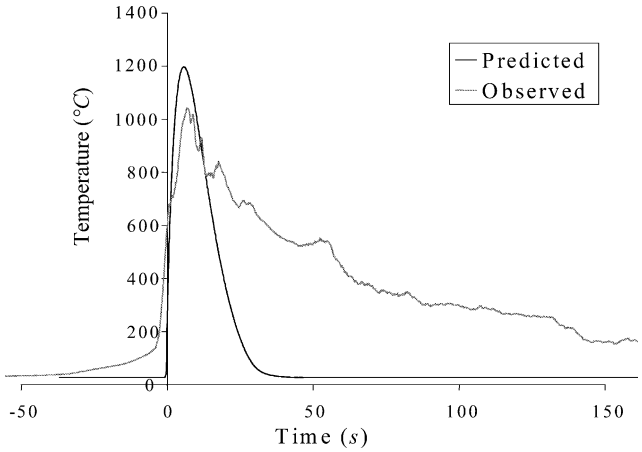

Fig. 10. Experimental and predicted temperature curves for a 10° slope and 2 m·s^{-1} wind speed.

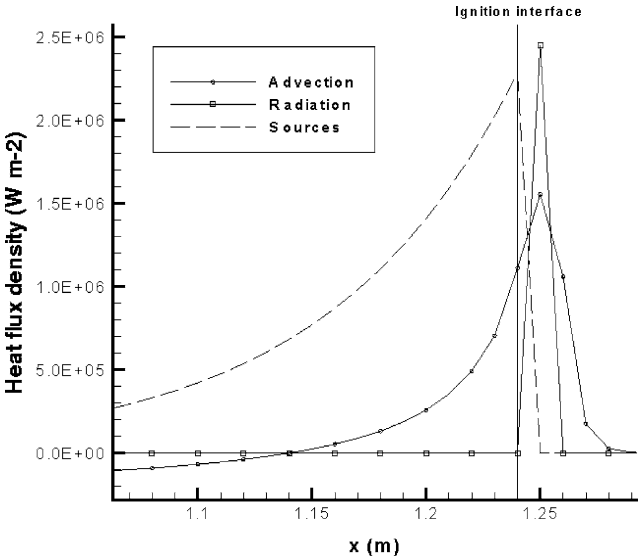

Fig. 11. Heat flux density of advection, radiation and sources along the fuel bed at a given time for no slope and 2 m·s^{-1} wind speed.

an overall agreement between predicted and observed rates of spread, even if the model underpredicts fire spread for the highest velocity of 3 m·s^{-1}. The agreement is quite good for all slopes considered when the wind velocity is lower than or equal to 2 m·s^{-1}. A substantial improvement is thus made if one considers that the previous radiative model was unable to depict this tendency accurately. Indeed, the results of the simplified-flow model are nearer to the observed results. Moreover, it provides a better prediction of the rate of fire spread which increases with increasing wind for a given slope. In Fig. 8, we can observe that the highest value of fire spread rate (3 m·s^{-1}) is better represented than for the radiative model as well. In Fig. 9, we notice that an increase in the predicted rate of spread with increasing slope is also provided, even if it remains lower than the increase observed in experimental values. Indeed, although it is roughly given for no slope, 5° and 10° slope, it is rather under-estimated for the 15° slope.

Above, we asserted that this under-prediction for winds of 3 m·s^{-1} and steep slopes was partially due to a poor modelling of radiation in the model [16]. Indeed, if one examines the temperature over time at a given point for a wind velocity of 2 m·s^{-1} and a 10° slope (cf. Fig. 10), it will be possible to note that radiation does not allow the model to describe the preheating that occurs ahead of the fire front (left-hand side of the curve), as observed in experimental curves. With regard to the other parts of the temperature curve, namely the maximum and cooling zones, they are poorly described by thermocouple measurements [26]. It is thus hazardous to discuss them. Nevertheless, it should be noted that measurements obtained using infrared thermal imaging yielded maximal temperatures (approximately 1200 °C for needle beds of the same type as those used in this study) which corresponds to the temperatures generated by the model [27]. The lack of preheating by radiative transfer in our modelling is best explained by examining Fig. 11, which describes the spatial distribution of both convection and radiation transfers along the fuel bed at a given time and for a wind velocity of 2 m·s^{-1} and no slope. It is clear that radiation is transferred to the first cell ahead of the fire front in an abrupt manner (cf. Eq. (8)). No preheating effect caused by radiation is obtained, whereas preheating by convection is described. However, despite this poor representation, neither energy transfer is negligible when the two are compared to each other. This would tend to confirm the results of other studies [28]. Including a long range radiation sub-model, such as that developed by Morandini et al. [29], will probably provide a better description of heat transfers in the fuel bed.

The thermal equilibrium assumption can provide further discrepancies. However, we set this hypothesis for the ex-

periments considered in the present study since a multiphase numerical investigation [25] has shown that the maximal difference between the two phases was roughly of 20% in the whole fuel layer. This assumption allowed us to represent the experimental tendencies correctly. Nevertheless, it is possible that other experimental configurations will reveal the necessity to model the gas phase and the solid phase temperatures separately, in much the same way as we have demonstrated that a simple description of the flow was missing in our model. But, following our modelling approach, we will not perform this study until the previous improvements (concerning radiation modelling and χ estimation) have proved to be insufficient. Another phenomenon that is of importance for high wind-driven fire spreads is the development of a mixed flow boundary layer above the fuel bed. It could explain to a great extent the discrepancy between the predicted and experimental rates of spread for a 3 $\mathrm{m{\cdot}s^{-1}}$ wind. Indeed, for high winds the flame is deflected and this boundary layer increases considerably radiative and convective transfers at the fuel surface.

6. Conclusions

In the present study we were able to develop a simple description of the flow while a fire spreads. This led us to enhance our semi-physical model. We thus defined a supplementary state variable in our modelling, namely the gas velocity in the combustion zone. In order to allow a simple formulation, we limited ourselves to a flow in one horizontal direction. This configuration was the only experimental one that allowed us to validate our approach. The main contribution of the model consists in its ability to describe physical behaviour that was not represented previously in our approach, such as the aspiration of cold gas by the flame and the abrupt decrease in gas velocity as it throws the combustion zone. In addition, this study allowed us both to obtain better predictions of fire spread rates than the radiative model and to provide an improved representation of experimental tendencies. We are thus able to assert that, by including a simplified flow, we improved the model's capacity to describe the physical phenomena involved in fire spread. We have also shown in which direction future efforts must be oriented to continue to improve the model. A further model improvement, however, will need to take long range radiation into consideration, since the model just describes the preheating of the unburned fuel through convective transfers. The development of a mixed flow boundary layer above the fuel bed have to be studied too. Indeed, it represents an important aspect of the high wind-driven fires as it affects the thermal balance at the fuel surface.

Finally, the present work will also permit to include in the model phenomena that have been neglected up to now, in particular the effect of cold gas aspiration in the reacting zone. It also represents a first step towards the development of flow in the two horizontal directions that we are currently studying in the hope of integrating it into the fire spread model. Finally, an additional valuable aspect of this study is that the simplified description of the aerodynamics applied to our model can be used within the framework of other semi-physical models based on a thermal balance.

Acknowledgements

The authors would like to thank Pr. J.M. Mendes-Lopes, Pr. J.M. Ventura, Dr. J.M. Amaral and Dr. L.M. Ripado for the provided experimental results they have obtained at the IST of Lisboa [18,26].

Appendix A. The semi-physical model

Due to the amount of physical phenomena and state variables involved in fire behaviour, and if we want to reach our goal which is to elaborate a forest fire simulator, it will be necessary to make some simplifying hypotheses in order to generate a comprehensive and simple model. These hypotheses lead us to combine these physical phenomena and to consider a thermal balance which provides the framework of the model. In order to develop such a thermal balance, elementary cells composed of soil and plant matter are defined. As a whole, these cells are considered to represent a thin, isotropic and homogenous medium equivalent to the litter. The energy transferred from a cell to the surrounding air is considered as being proportional to the difference between the temperature of a cell and the ambient temperature. Combustion reaction is assumed to occur above a threshold temperature (T_{ig}). Above this threshold, we assume that the fuel mass decreases exponentially and that the quantity of heat generated per unit fuel mass is constant. The heat transferred between a cell and its neighbouring cells is caused by three mechanisms: radiation, convection and conduction. We assume that these exchanges can be represented by a single equivalent diffusion term, under no slope and no wind conditions. However, due to obvious geometric reasons, a supplementary radiation term was considered for upslope and low upwind fires. In order to evaluate this term, we consider the flame as being a vertical radiant surface, the temperature of which is equal to the temperature of the burning cell located below it. This temperature is given by the model. By using a Stefan–Boltzmann law, we assume that the radiant heat flux is proportional to T^4 and that it prevails over a short distance d. In a previous study [14], we established that an unburned cell in the direction of the slope receives an additional radiant heat flux from a burning cell directly before it, this flux being proportional to the cosine of the angle θ located between the normal of the front and the direction of the slope:

$$R = P(\phi)\cos(\theta)T^4(x-d,y,t) \tag{A.1}$$

where $T(x-d,y,t)$ is the temperature of the burning cell located just before the unburned cell under consideration,

$P(\phi)$ being a function of the flame tilt angle, the emissivity of the flame, the absorptivity of the fuel and the view factor. It is not reasonable to take all these parameters into consideration in our macroscopic approach. Hence, $P(\phi)$ has been determined by basing on laboratory fire experiments from an empirical law [16]. For upwind fires, a convective term was also added to the model [17]. We obtained the following model of fire spread:

$$\frac{\partial T}{\partial t} + k_v \vec{V}_g \cdot \vec{\nabla} T = -k(T - T_a) + K\Delta T - Q\frac{\partial s_k}{\partial t} + R \tag{A.2}$$

$R = 0, \qquad s_k = s_{k0}\,\mathrm{e}^{-\gamma(t-t_{ig})}$

for a burning cell

$R = P(\phi)\cos(\theta)T^4(x-d, y, t), \qquad s_k = s_{k0}$

for an inert cell ahead of the fire front

$R = 0, \qquad s_k = s_{k0}$

for an unburned cell somewhere else

$\vec{V}_g = \vec{V}_\infty$

on the whole domain

With the boundary and initial conditions:

$T = T_a$

at the boundaries far from the fire

$T(x, y, t = 0) = T_a$

for an unignited cell at time zero

$T(x, y, t = 0) = T_{ig}$

for an ignited cell at time zero

where t_{ig} is the time for which $T = T_{ig}$. The model parameters (k, K, Q and γ) are determined using the experimental temperature measurements over time for a fire spreading in a linear fashion under no slope and no wind conditions [13]. Due to our approach, these parameters are fuel-dependent and must therefore be identified for each fuel. Thus, the usual fuel descriptors such as mass per unit area, particle size, compactness, physical–chemical properties and moisture content are intrinsically taken into account. $P(\phi)$ has been determined using the following empirical law [16]:

$$P(\phi) = p_0 \sin^4(\phi) \tag{A.3}$$

where p_0 is a constant and ϕ represents the flame tilt angle under upslope and wind-aided conditions. With regard to ϕ, a simple relation was used to determine this term: this angle was considered as being the sum of the tilt angle due to slope (equal to the slope angle) and the tilt angle due to wind effects (estimated from the competition between wind velocity and buoyancy flow velocity under no slope condition, both taken at mid-flame [16]). Concerning the convective term, we assumed, as a first step, that the maximum wind velocity $\vec{V}_\infty$ could be used in Eq. (A.1) to roughly represent wind velocity $\vec{V}_g$, present over the entire fire spread domain. The coefficient k_v was deduced from the multiphase model, assuming that the gas is perfect, that its specific heat remains constant and that the quasi-isobaric approximation is valid [17]. We thus obtain the following relation:

$$k_v = \frac{\alpha_g \rho_a \delta C_{p,g}}{m_{eq}} \cdot \frac{T_a}{T} = k_v^* \cdot \frac{T_a}{T} \tag{A.4}$$

in which m_{eq} is the surface thermal mass of the semi-physical medium equivalent to the litter, defined as the sum of the fuel bed thermal mass and of the ground thermal mass. It should be noted that, for the experiments considered in this paper, the thermal mass of the ground represents 90% of m_{eq}.

References

[1] R.O. Weber, Modelling fire spread through fuel beds, Prog. Energy Combust. Sci. 17 (1990) 67–82.

[2] A.G. McArthur, Weather and grassland fire behaviour, Australian Forest Timber Bureau Leaflet 100 (1966).

[3] R.C. Rothermel, A mathematical model for predicting fire spread in wildland fuels, USDA Forest Service Res. Paper INT-115, 1972.

[4] F.A. Albini, A model for fire spread in wildland fuels by radiation, Combust. Sci. Technol. 42 (1985) 229–258.

[5] A.M. Grishin, Mathematical Modeling of Forest Fires and New Methods of Fighting Them, Publishing House of the Tomsk State University, 1997, Albini Ed. Chapter 1, pp. 81–91.

[6] M. Larini, F. Giroux, B. Porterie, J.C. Loraud, A multiphase formulation for fire propagation in heterogeneous combustible media, Internat. J. Heat Mass Transfer. 41 (1997) 881–897.

[7] F. Giroux, Contribution to fire spreading modelling: Multiphase approach of forest fires, development of a propellant fire in a semi-confined medium. Thesis, Doctorate of University, University of Provence, IUSTI, Aix-Marseille-I, France, 1997 (in French).

[8] J.L. Dupuy, M. Larini, Fire spread through a porous forest fuel bed: A radiative and convective model including fire-induced flow effects, Internat. J. Wildland Fire 9 (2001) 155–172.

[9] P.L. Andrews, BEHAVE: Fire behavior prediction and fuel modeling subsystem, USDA Forest Service Report INT-194, Intermountain Research Station, Ogden, UT 84401, 1986.

[10] M.A. Finney, FARSITE: Fire area simulator—Model development and evaluation, Res. Pap. RMRS-RP-4, Ogden, Utah: USDA, Forest Service, Rocky Mountains Research Station, 1998.

[11] R.R. Linn, F.H. Harlow, Use of transport models for wildfire behaviour simulations, in: Proceedings of III Internat. Conf. on Fire Research, 1, 1998, Coimbra, Portugal, pp. 363–372.

[12] N. Lymberopoulos, T. Tryfonopoulos, F.C. Lockwood, The study of small and meso-scale wind field—Forest fire interaction and buoyancy effects using the AIOLOS-F simulator, in: Proceedings of III Internat. Conf. on Fire Research, 1, 1998, Coimbra, Portugal, pp. 405–418.

[13] J.H. Balbi, P.A. Santoni, J.L. Dupuy, Dynamic modelling of fire spread across a fuel bed, Internat. J. Wildland Fire 9 (1999) 275–284.

[14] P.A. Santoni, J.H. Balbi, J.L. Dupuy, Dynamic modelling of upslope fire growth, Internat. J. Wildland Fire 9 (1999) 285–292.

[15] L. Ferragut, M.I. Asensio, R. Montenegro, G. Plaza, F. Winter, F.J. Serón, A model for fire simulation in landscape, Comput. Fluid Dyn. (1996) 111–116.

[16] F. Morandini, P.A. Santoni, J.H. Balbi, Analogy between wind and slope effects on fire spread across a fuel bed—Modelling and validations, in: Proceedings of 3rd Internat. Sem. on Fire and Explosion Hazards, Edinburgh, Scotland, UK, 2000.

[17] A. Simeoni, P.A. Santoni, M. Larini, J.H. Balbi, Proposal for theoretical improvement of semi-physical forest fire spread models thanks to a

multiphase approach: Application to a fire spread model across a fuel bed, Combust. Sci. Technol. 162 (2001) 59–84.
[18] J.M. Mendes-Lopes, J.M. Ventura, J.M. Amaral, Rate of spread and flame characteristics in a bed of pine needles, in: Proceedings of III Internat. Conf. on Fire Research, 1, 1998, Coimbra, Portugal, pp. 497–511.
[19] F.A. Albini, A model for the wind-blown flame from a line fire, Combust. Flame 43 (1981) 155–174.
[20] M. Guijarro, C. Hernando, J.A. De Los Santos, C. Diez, Forest fire behaviour in the wind tunnel, Intermed. Report Efaistos Proj. (1998).
[21] R. Comolet, Mécanique Expérimentale des Fluides, Masson 4, Paris, 1982, pp. 216–230.
[22] R.O. Weber, Toward a comprehensive wildfire spread model, Internat. J. Wildland Fire 1 (1991) 245–248.
[23] H.M. Cekirge, Propagation of fire fronts in forests, Comput. Math. Appl. 4 (1978) 325–332.
[24] S.V. Patankar, Numerical Heat Transfer and Fluid Flow, Hemisphere, 1980, 198 p.
[25] B. Porterie, D. Morvan, J.C. Loraud, M. Larini, A multiphase model for predicting line fire propagation, in: Proceedings of III Internat. Conf. on Fire Research, 1, 1998, Coimbra, Portugal, pp. 343–360.
[26] J.M. Ventura, J.M. Mendes-Lopes, L.M. Ripado, Temperature-time curves in fire propagating in beds of pine needles, in: Proceedings of III Internat. Conf. on Fire Research, 1, 1998, Coimbra, Portugal, pp. 699–711.
[27] E. Den Breejen, M. Roos, K. Schutte, J.S. De Vries, H. Winkel, Infrared measurements of energy release and flame temperatures of forest fires, in: Proceedings of III Internat. Conf. on Fire Research, 1, 1998, Coimbra, Portugal, pp. 517–532.
[28] P.J. Pagni, T.G. Peterson, Flame spread through porous fuels, in: Proceedings of 14th Internat. Sympos. on Combus, The Combustion Institute, England, 1973, pp. 1099–1107.
[29] F. Morandini, P.A. Santoni, J.H. Balbi, The contribution of radiant heat transfer to laboratory scale fire spread under the influences of wind and slope, Fire Safety J. 36 (2001) 519–543.